This is the author's version of an article that has been published in: *2018 First International Workshop on Mobile Terahertz Systems (IWMTS)*, IEEE, 2018, pp. 1-4. Changes were made to this version by the publisher prior to publication. The final version of record is available at: https://doi.org/10.1109/IWMTS.2018.8454700

Millimeter-wave Signal Generation and Detection via the same Triple Barrier RTD and on-chip Antenna

K. Arzi, A. Rennings, D. Erni, N. Weimann, W. Prost
University of Duisburg-Essen
Faculty of Engineering, Duisburg, Germany
Khaled.arzi@uni-due.de

S. Suzuki, M. Asada
Tokyo Institute of Technology
Interdisciplinary Graduate School of Science and Engineering, Tokyo, Japan

***Abstract*— Signal generation and detection at mm-wave frequencies via a single chip size component is demonstrated. The monolithic integration consists of high current density Triple Barrier Resonant Tunneling Diode into a slot antenna. The asymmetrical current voltage characteristic of the Triple Barrier Resonant Tunneling Diode enables signal detection at zero bias and signal generation at forward bias within the regime of negative resistance. Signal generation and detection at above 250 GHz are experimentally demonstrated.**

Keywords—Resonant tunneling diode; millimeter-wave detector; rectification; THz signal

I. INTRODUCTION

The chip-size generation (sub-)mm wave signal at high power efficiencies is a prerequisite for the exploitation of these frequency bands for mobile applications. In addition, most of the intended mobile applications such as communication, material detection, and ultra-high spatial resolution radar require both signal generation and detection, respectively.

The Resonant Tunneling Diode (RTD) provides compact and energy efficient semiconductor based fundamental mode sources at THz frequencies up to almost 2 THz at room temperature [1] [2]. To date, the RTD is the fastest semi-conductor-based electronic device [1]. A modification of the RTD by adding an additional third barrier forms a triple barrier RTD (TB-RTD). The TB-RTD has been used to provide unsymmetrical current voltage characteristics enabling additional detector applications [3]. This makes the TB-RTD a promising candidate for both, THz signal transmitter and detector based on the advantage of high current density and small parasitic capacitance [3-5]. Recently, simulation works predicted that the integration of the TB-RTD in on-chip antenna [6, 7] result into the detection and transmission of signals in the THz frequency regime.

In this work we present the design of high current density TB-RTD (> 400 kA/cm^2) with a wide negative differential resistance regime (NDR) in the forward direction and a very non-linear behavior at zero-bias. This device will be monolithically integrated into a slot antenna. Signal generation and detection just by changing the bias with the identical device combination is demonstrated at frequencies well above 250 GHz.

This work is co-funded by the Deutsche Forschungsgemeinschaft within the Collaborative Research Centre SFB TRR 196 MARIE C02 / C05 and the European Innovative Training Network 765426 TeraApps.

II. LAYER DESIGN AND PROCESSING

Modifying the RTD structure by adding an additional thin barrier to the device creates a second quantum well. The well widths and barrier heights are designed to provide asymmetric and nonlinear current voltage characteristics. Biasing the device in the forward direction, only enables resonance between the quantum levels in both wells providing sequential tunneling for a wide NDR and comparable current densities as compared to double barrier RTDs. Biasing the device in the reverse direction leads to a misalignment between the levels in the quantum wells such that the resonant tunneling is inhibited (c.f. Fig. 2). Therefore, the TB-RTD can be used for both, signal generation and detection, respectively.

The layer stack of the TB-RTD is presented in TABLE I. The layer stack has been grown by molecular beam epitaxy on semi-insulation InP-substrate. The details for the growth and processing of high current density tunneling diodes are reported elsewhere [8, 9].

TABLE I. LAYER SEQUENCE OF THE FABRICATED TB-RTD

Function	Material	Thickness [nm]	Doping [10^{18}cm^{-3}]
Contact layer	$In_{0.7}Ga_{0.3}As$	8	37.4
Contact layer	InGaAs	100	37.4
Grading layer	InGaAs >	50	37.4 to 1
Spacer	InGaAs	1.17	
Barrier	AlAs	1.7	
Well, smoothing	InGaAs	1.46	
1st Well	InAs	1.21	n. i. d.
Well, smoothing	InGaAs	1.46	
Barrier	AlAs	1.7	
Well, smoothing	InGaAs	1.46	
2nd Well	InAs	2.42	
Well, smoothing	InGaAs	1.46	
Barrier	InAlAs	1.7	
Spacer	InGaAs	1.17	
Grading layer	InGaAs <	50	1 to 37.4
Contact layer	InGaAs	300	37.4
Substrate	s. i. InP (100)	350 µm	Fe

Heavily Si-doped InGaAs contact layers are used to provide high current densities with low resistive contacts to the intrinsic

device. Additionally an 8 nm height InGaAs layer with higher indium fraction is used to improve the metal semiconductor interface for the top contacts. The intrinsic device is placed between the spacer layers as shown in Table 1. The quantum wells are formed with an InGaAs/InAs/InGaAs layer stack. The wells width and barrier height are designed to achieve a current blocking behavior in the reverse direction and resonant tunneling in the forward direction.

Optical lithography, dry and wet etching and Ti/Pt/Au/Ni lift-off technology are used for device processing [8]. A schematic structure of the device and a SEM micrograph are shown in Fig. 1.

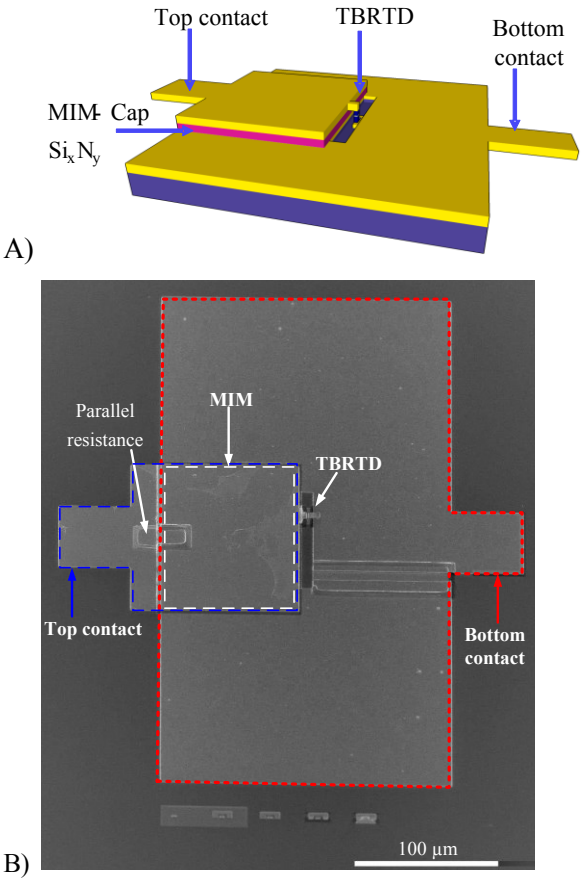

Fig. 1. Integration of the TB-RTD in a slot antenna. A) Side view of the schematic structure B) SEM micrograph of the oscillator at the top view.

To suppress potential parasitic oscillations at low frequencies a parallel stabilization resistance is used. A multiple TB-RTD mesa design is employed to minimize the parasitic series resistance indispensable at very high current density [9]. For device characterization TB-RTD with a coplanar waveguide contacts are fabricated on the wafer, separately.

III. DEVICE CHARACTERIZATION

A. DC- Characterization:

The current voltage characteristic of the TB-RTD is presented in figure 2. The behavior of the conduction band edge of the TB-RTD in the forward and reverse direction is schematically presented as inset in figure 2.

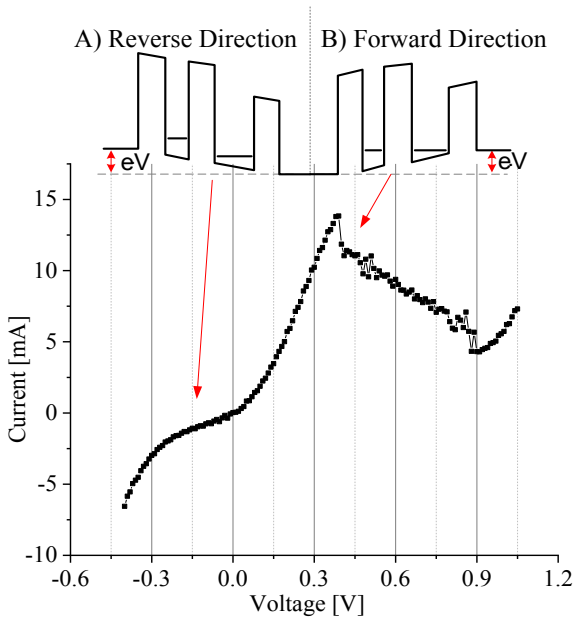

Fig. 2. Current-Voltage characteristics of TB-RTD (A=3µm²´). The insets depict the conduction band edge of the TB-RTD at reverse (A) and forward (B) bias, respectively.

In forward direction a steep current increase up to peak current of 420 kA/cm^2 is observed. The NDR shows a peak to valley current ratio of 3.3. The energy of the discrete levels in the well defines the peak voltage and can be modified by changing the width of the wells. In the current TB-RTD design, both, the peak voltage and the current density, respectively, remain at comparable levels as compared to double barrier RTD.

In the reverse direction a current blocking behavior is observed for small voltages. For voltages higher than 0.3 V an increase in the thermionic current can be observed. A rectification factor G of the device at small voltages is shown in Fig. 3. To investigate the rectification factor from the DC-Characteristics the following equation is used:

$$G = \frac{J_F(V_{pos})}{J_R(V_{neg})}, |V_{pos}| = |V_{neg}|$$

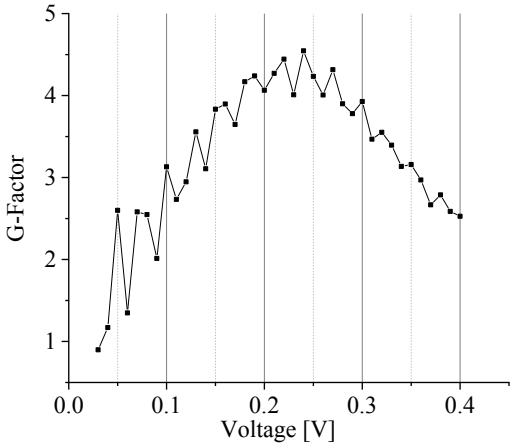

Fig. 3. The rectification factor G vs. bias voltage.

The TB-RTD approach provides several parameters for performance optimization with a high degree of freedom, to suppress the thermionic current in the reverse direction and improve the rectification factor: Material, doping profile in the contacts and the thickness of the barriers and wells can be adjusted [10].

B. RF- Characterization:

The high frequency performance of the device is investigated with a vector network analyzer. S-parameter measurements have been performed for frequencies up to 47 GHz. The measured data were de-embedded using open and short structures fabricated on wafer. The analyses of the device are carried out using a simple equivalent circuit of the RTD as shown in figure 4.

The capacitance C_{RTD} of the device at zero bias was extracted to be 5.3 fF/µm^2 and decreases at lower voltages due to the increase of the depletion layer. At positive voltages the depletion layer is reduced which increases somewhat the capacitance. Therefore, the oscillation frequency and detection frequencies of the device will vary with bias voltage. Accurate measurements in the NDR without stabilization [11] are very challenging due to the emergent oscillations. The capacitance of the device in this particular region is thus approximated to C_{RTD}(NDR) = 6 fF/µm^2.

IV. TB-RTD INTEGRATION IN ANTENNA

Fig. 4 presents the equivalent circuit used for the oscillator. The oscillations conditions of such oscillator are given by:

$$Re\{Y_{TBRTD}(\omega_{osc})\} + Re\{Y_A(\omega_{osc})\} < 0 \quad (1)$$

$$Im\{Y_{TBRTD}(\omega_{osc})\} + Im\{Y_A(\omega_{osc})\} = 0 \quad (2)$$

Biasing the TB-RTD in the NDR with a $|G_{TBRTD}| > |G_A|$ can fulfill the requirement of compensating the losses of the antenna. To fulfill the second requirement for conjugate matching the antenna must have an inductive behavior over the requested frequency range. Therefore the slot antenna is not designed for resonance oscillation but designed to provide an inductance behavior. The capacitance behavior of the slot antenna at this design can be neglected.

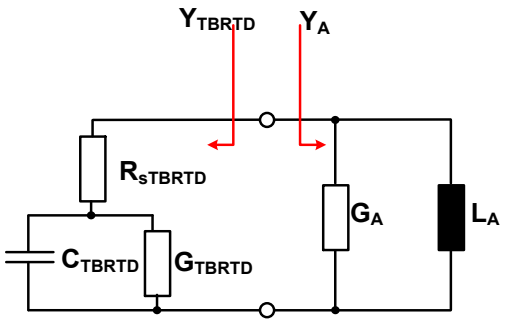

Fig. 4. Equivalent circuit of the TB-RTD and slot antenna.

The simulation of the slot antenna is carried out using the Advanced Design System (ADS) software. The S_{11} results of the simulation are used to characterize the antenna equivalent circuit. Due to the fact that the antenna is not designed for resonant oscillation the equivalent circuit used contains only an inductance and a resistance for the antenna losses. The dimensions of the slot are the crucial factor for the inductance value and hence for the oscillation frequency. With slot dimensions of L = 80 µm and W = 10 µm and feeding position of 15 µm shift from the center of the slot, the extracted values are as follows: $L_A = 17.5\,pH$ *and* $G_A = 3.2\,mS$. To suppress parasitic oscillation at lower frequencies due to the resonance formed by external circuits including biasing lines, a resistance parallel to the RTD is used as shown in figure 1.

V. OSCILLATOR AND DETECTOR MEASUREMENTS

As discussed above the advantage of the TB-RTD is the capability of designing one device that can be used for signal generation and detection depending on its biasing point. We start with biasing the device in the NDR while measuring its oscillations frequencies. The measurement setting is shown in Fig. 5.

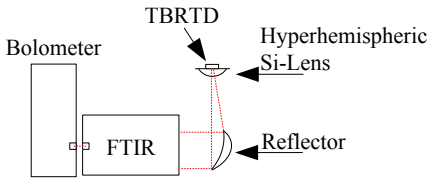

Fig. 5. Measurement setting for oscillation frequency measurement.

A liquid He-cooled Si composite bolometer was used as detector and the oscillation spectra were measured by a Fourier transform IR spectrometer (FTIR). The biasing is carried out on wafer with DC probes. By Biasing the TB-RTD in the NDR yields an output signal oscillation at 260 GHz (cf. Fig. 6). The measurement was carried out in the pulsed mode with a lock-in technique to eliminate the surrounding noise. The pulse width and repetition rate are 0.3 mS and 300 Hz. The changes due to the pulsed mode are negligibly.

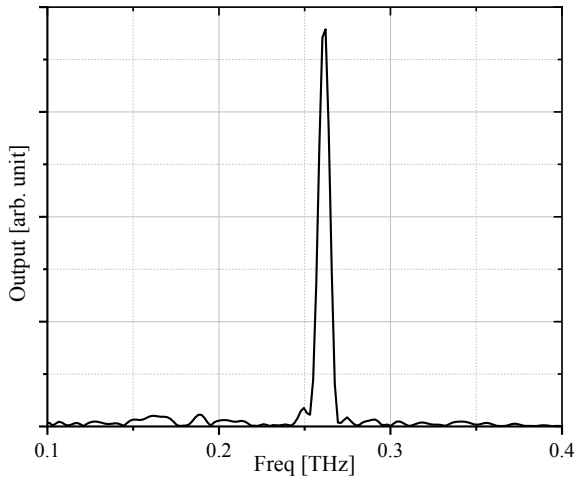

Fig. 6. Measured spectrum with FTIR of the output signal of the TB-RTD biased in the NDR.

To measure the accurate output power of the device the signal was focused on the input of the bolometer without the FTIR. The determined effective output power of the device is

at ~ 92 µW. The measurement includes some errors due to the insufficient alignment of the setup.

To measure the detection capability of the device a second measurement setup was used, where the bolometer is replaced by a signal generator. An optical chopper was placed between the focusing lens and the signal generator. The detected voltage was measured with a lock-in technique. The output frequency is swept from 250 GHz to 320 GHz as shown in Fig. 7. The average signal power of the radiated signal is at -36 dBm.

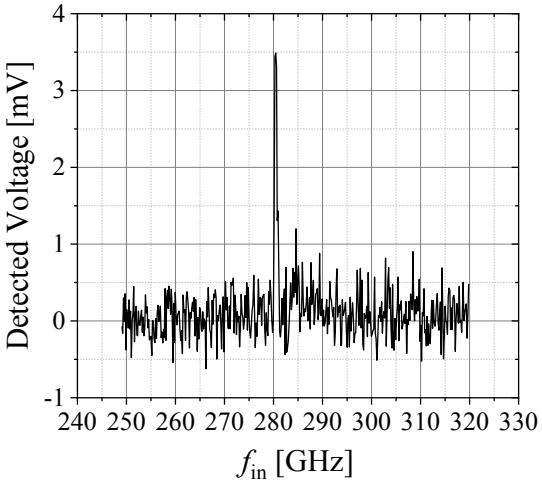

Fig. 7. Measured voltage with locking technique for the TB-RTD biased at zero volt.

A detection peak is at f ~ 280 GHz as shown in Fig. 7. The peak power is also dependent on the radiated signal power.

VI. CONCLUSION

In this work we presented the on-chip integration of a high current density TB-RTD into a slot antenna for both, signal generation and detection. The oscillator design was carried out for oscillation and detection of signals > 250 GHz. The high current densities combined with a small parasitic capacitance of the TB-RTD make it a valuable candidate also for higher THz signal generation and sensitive detection.

ACKNOWLEDGMENT

The author K. Arzi thanks Prof. Asada and Prof. Suzuki for giving him the opportunity of a short term scientific mission to their labs at the Tokyo Institute of Technology. During this stay K. Arzi performed the RF measurements and enjoyed many fruitful discussions.

REFERENCES

[1] R. Izumi, S. Suzuki and M. Asada, "1.98 THz resonant-tunneling-diode oscillator with reduced conduction loss by thick antenna electrode," *2017 42nd International Conference on Infrared, Millimeter, and Terahertz Waves (IRMMW-THz)*, Cancun, 2017, pp. 1-2. doi: 10.1109/IRMMW-THz.2017.8066877

[2] H. Kanaya, R. Sogabe, T. Maekawa, S. Suzuki, and M. Asada, "Fundamental oscillation up to 1.42 THz in resonant tunneling diodes by optimized collector spacer thickness," J. Infrared, Millimeter and Terahertz Waves, vol. 35, pp. 425-431, May, 2014.

[3] R. Sekiguchi, Y. Koyama, and T. Ouchi, „Subterahertz oscillations from triple-barrier resonant tunneling diodes with integrated patch antennas", Applied Physics Letters, vol. 96, Issue 6, February2010

[4] M. Suhara *et al*., "Analysis of terahertz zero bias detectors by using a triple-barrier resonant tunneling diode integrated with a self-complementary bow-tie antenna," *70th Device Research Conference*, University Park, TX, 2012, pp. 77-78.
doi: 10.1109/DRC.2012.6256934

[5] G. Keller, A. Tchegho, B. Münstermann, W. Prost, F. J. Tegude and M. Suhara, "Characterization and modeling of zero bias rf-detection diodes based on triple barrier resonant tunneling structures," *2013 International Conference on Indium Phosphide and Related Materials (IPRM)*, Kobe, 2013, pp. 1-2. doi: 10.1109/ICIPRM.2013.6562641

[6] A. Rennings, B. Sievert, W. Liu, K. Arzi, W. Prost and D. Erni, "Broadband millimeter-wave detector based on triple-barrier resonant tunneling diode and tailored archimedean spiral antenna," *2017 IEEE Asia Pacific Microwave Conference (APMC)*, KUALA LUMPUR, Malaysia, 2017, pp. 775-778.
doi: 10.1109/APMC.2017.8251563

[7] M. Suhara *et al*., "Analysis of terahertz zero bias detectors by using a triple-barrier resonant tunneling diode integrated with a self-complementary bow-tie antenna," *70th Device Research Conference*, University Park, TX, 2012, pp. 77-78.
doi: 10.1109/DRC.2012.6256934

[8] K. Arzi, G. Keller, A. Rennings, D. Erni, F. J. Tegude and W. Prost, "Frequency locking of a free running resonant tunneling diode oscillator by wire-less sub-harmonic injection locking," *2017 10th UK-Europe-China Workshop on Millimetre Waves and Terahertz Technologies (UCMMT)*, Liverpool, 2017, pp. 1-4.
doi: 10.1109/UCMMT.2017.8068485

[9] A. Tchegho *et al*., "Scalable high-current density RTDs with low series resistance," *2010 22nd International Conference on Indium Phosphide and Related Materials (IPRM)*, Kagawa, 2010, pp. 1-4.
doi: 10.1109/ICIPRM.2010.5516377

[10] G. Keller, A. Tchegho, B. Münstermann, W. Prost and F. J. Tegude, "Sensitive high frequency envelope detectors based on triple barrier resonant tunneling diodes," *2012 International Conference on Indium Phosphide and Related Materials*, Santa Barbara, CA, 2012, pp. 36-39. doi: 10.1109/ICIPRM.2012.6403312

[11] L. Wang, J. M. L. Figueiredo, C. N. Ironside and E. Wasige, "DC Characterization of Tunnel Diodes Under Stable Non-Oscillatory Circuit Conditions," in *IEEE Transactions on Electron Devices*, vol. 58, no. 2, pp. 343-347, Feb. 2011.
doi: 10.1109/TED.2010.2091507

DOI: 10.1109/IWMTS.2018.8454700
URN: urn:nbn:de:hbz:465-20221121-135021-7

This is the author's version of this article: K. Arzi et al., "Millimeter-wave Signal Generation and Detection via the same Triple Barrier RTD and on-chip Antenna," *2018 First International Workshop on Mobile Terahertz Systems (IWMTS)*, IEEE, 2018, pp. 1-4. Changes were made to this version by the publisher prior to publication. The final version of record is available at: https://doi.org/10.1109/IWMTS.2018.8454700